Integrated intelligent computing with neuro-swarming solver for multi-singular fourth order nonlinear Emden-Fowler equation

Zulqurnain Sabir[1], Muhammad Asif Zahoor Raja[2, 3], Juan L.G. Guirao[4], Muhammad Shoaib[5]

[1]Department of Mathematics and Statistics, Hazara University, Mansehra, Pakistan
[a]Email: zulqurnain_maths@hu.edu.pk
[2]Future Technology Research Center, National Yunlin University of Science and Technology, 123 University Road, Section 3, Douliou, Yunlin 64002, Taiwan, R.O.C.
[3]Department of Electrical and Computer Engineering, COMSATS University Islamabad, Attock Campus, Attock 43600, Pakistan
Email: rajamaz@yuntech.edu.tw

[4]Department of Applied Mathematics and Statistics, Technical University of Cartagena, Hospital de Marina 30203-Cartagena, Spain

Email: juan.garcia@upct.es

[5]Department of Mathematics, COMSATS University Islamabad, Attock Campus, Attock 43600, Pakistan

Email: dr.shoaib@cuiatk.edu.pk

Abstract: In the present work, a novel neuro-swarming based heuristic solver is established for the numerical solutions of fourth order multi-singular nonlinear Emden-Fowler (FO-MS-NEF) model by using the function estimate capability of artificial neural networks (ANNs) modelling together with the global application of particle swarm optimization (PSO) enhanced by local search active set (AS) approach, i.e., ANN-PSO-AS solver. The design stimulation for the ANN-PSO-AS scheme for a numerical solver originates with an intention to present a viable, consistent and precise configuration that associates the ANNs strength under the optimization of unified soft computing backgrounds to tackle with such stimulating models for the FO-MS-NEF equation. The proposed ANN-PSO-AS solver is applied for three different variants of FO-MS-NEF equations. The comparison of the obtained results with the true solutions calmed its correctness, effectiveness, and robustness that is further validated with in-depth statistical investigations.

Keywords: Multi-Singular; Fourth order Emden-Fowler model; Artificial neural networks; Particle swarm; Active set scheme.

1. Introduction

The study nonlinear singular system governed with Emden–Fowler (EF) equation is considered to be very significant due to its vast applications in relativistic mechanics, evolution of populations, fluid mechanics, pattern construction and chemical reactor models [1-5]. The EF equation is historical and famous because of the singularity at the origin. These types of singular equations have been applied in the study of electromagnetic theory, oscillating magnetic fields, density state of gaseous star, stellar structure, isothermal gas spheres, catalytic diffusion reactions, electromagnetic theory, quantum/classical mechanics, and continuous isotropic media [6-12]. The standard form of the second order EF equation is written as [13–14]:

$$\frac{d^2U}{d\tau^2}+\frac{\Psi}{\tau}\frac{dU}{d\tau}+h(\tau)g(U)=0,$$
$$U(0)=a,\ \frac{dU(0)}{d\tau}=0. \quad \textbf{(1)}$$

The equation (1) becomes the Lane–Emden (LE) model for $h(\tau)=1$ and written as:

$$\frac{d^2U}{d\tau^2}+\frac{\Psi}{\tau}\frac{dU}{d\tau}+g(U)=0,$$
$$U(0)=a,\ \frac{dU(0)}{d\tau}=0, \quad \textbf{(2)}$$

where $h(\tau)$ and $g(U)$ are the functions of τ and U, respectively. The shape factor is denoted by Ψ. The objective of the present research is to treat the fourth order multi-singular nonlinear Emden-Fowler (FO-MS-NEF) system numerically. The literature form of the FO-MS-NEF equation is given as [15]:

$$\frac{d^4U}{d\tau^4}+\frac{\Psi_1}{\tau}\frac{d^3U}{d\tau^3}+\frac{\Psi_2}{\tau^2}\frac{d^2U}{d\tau^2}+\frac{\Psi_3}{\tau^3}\frac{dU}{d\tau}+h(\tau)g(U)=0,$$
$$U(0)=A,\ \frac{dU(0)}{d\tau}=0, \frac{d^2U(0)}{d\tau^2}=\frac{d^3U(0)}{d\tau^3}=0, \quad \textbf{(3)}$$

where $g(U)$ and $h(\tau)$ are the functions of U and τ, while the shape factors are Ψ_1, Ψ_2 and Ψ_3. To find the solutions of the EF and LE models given in equations (1), (2) and (3) are not easy due to singular points and only a few deterministic numerical techniques have been applied to solve such models [16-19]. All these reported schemes have their individual perks, significance and performance, as well as, limitations and demerits. Alongside, these conventional techniques, numerical solvers used the heuristic computing schemes, which seems proficient and capable to incorporate in the field of singular models by functioning the universal approximation competence of artificial neural networks (ANNs) together with the optimization of local/global based search schemes [20-25]. Few recent applications are Bratu type nonlinear systems [26], electrically conducting solid models [27], financial market prediction models [28], Bagley-Torvik equations in fluid dynamics [29], forecasting of summer precipitation [30], prey-predator models [31], nonlinear reactive transport model representing the soft tissues dynamics [32], nonlinear stiff singular systems governed with Thomas-Fermi model [33], singular periodic differential model [34], nonlinear electric circuit system [35], nonlinear multi-singular nonlinear models [36], elliptic partial differential equations [37], HIV infection model [38], nonlinear singular functional differential model [39-40], corneal shape eye surgery model [41], heat conduction system in human head [42], mosquito dispersal model [43], mathematical model of micropolar fluid flow with thermal effects in a permeable walled channel [44] and nanotechnology [45]. Inspired from these contributions, the authors presented the function approximation competence of artificial neural network (ANN) modelling together with the global based optimization appliance of particle swarm optimization (PSO) enhanced by a local search active set (AS) approach, i.e., ANN-PSO-AS scheme. The prime characteristics of the proposed ANN-GA-AS scheme are concisely given as:

- An innovative application of integrated solver ANN-PSO-AS is designed for the numerical results of the FO-MS-NEF model.
- Closely matching outcomes of the proposed ANN-PSO-AS scheme from the reference solutions for all examples of the FO-MS-NEF model based problems proven the worth and value in terms of precision and convergence.
- Verification of performance is endorsed from the statistical investigation on multiple trials of ANN-PSO-AS using the performance metrics of Theil's Inequality Coefficient (TIC), Variance Account For (VAF) and Nash Sutcliffe Efficiency (NSE).
- Beside the reasonable precise results for nonlinear FO-MS-NEF system, easy understanding, robustness, smooth operations, comprehensive applicability and stability are other esteemed merits.

The rest parts of this work are ordered as follows: Section 2 describes the proposed methodology. Section 3 shows the mathematical form of the statistical indices. Section 4 presents the detailed results and discussions. The conclusion together with future research direction is reported in the last Section.

2. Methodology

The proposed ANN-PSO-AS scheme is divided into two segments to show the numerical outcomes of the FO-MS-NEF system.

- Introduced a merit function using the differential model and corresponding initial conditions.
- The hybrid form of the designed ANN-PSO-AS scheme is presented.

2.1 ANN modeling

The structures for the ANNs have been proposed by many researchers to explain the linear/nonlinear classifications arising in different application of potential significance [46-48]. The ANN feed-forward models used to approximate the results of continuous mappings along with its derivatives by taking the log-sigmoid merit function $p(\tau)=\left(1+\mathrm{e}^{-\tau}\right)^{-1}$ is given as:

$$\begin{aligned}
\hat{U}(\tau) &= \sum_{i=1}^{k} l_i p(w_i\tau + b_i) = \sum_{i=1}^{k} l_i \left(1+e^{-(w_i\tau+b_i)}\right)^{-1}, \\
\frac{d\hat{U}}{d\tau} &= \sum_{i=1}^{k} l_i \frac{d}{d\tau} p(w_i\tau + b_i) = \sum_{i=1}^{k} l_i w_i e^{-(w_i\tau+b_i)} \left(1+e^{-(w_i\tau+b_i)}\right)^{-2}, \\
\frac{d^2\hat{U}}{d\tau^2} &= \sum_{i=1}^{k} l_i \frac{d^2}{d\tau^2} p(w_i\tau + b_i) = \sum_{i=1}^{k} l_i w_i^2 \left(2e^{-2(w_i\tau+b_i)} \left(1+e^{-(w_i\tau+b_i)}\right)^{-3} - e^{-(w_i\tau+b_i)} \left(1+e^{-(w_i\tau+b_i)}\right)^{-2}\right), \\
\frac{d^3\hat{U}}{d\tau^3} &= \sum_{i=1}^{k} l_i \frac{d^3}{d\tau^3} p(w_i\tau + b_i) = \sum_{i=1}^{k} l_i w_i^3 \left(\begin{array}{l} 6e^{-3(w_i\tau+b_i)} \left(1+e^{-(w_i\tau+b_i)}\right)^{-4} - 6e^{-2(w_i\tau+b_i)} \left(1+e^{-(w_i\tau+b_i)}\right)^{-3} \\ +e^{-(w_i\tau+\gamma_i)} \left(1+e^{-(w_i\tau+\gamma_i)}\right)^{-2} \end{array}\right), \\
\frac{d^4\hat{U}}{d\tau^4} &= \sum_{i=1}^{k} l_i \frac{d^4}{d\tau^4} p(w_i\tau + b_i) = \sum_{i=1}^{k} l_i w_i^4 \left(\begin{array}{l} 24e^{-4(w_i\tau+b_i)} \left(1+e^{-(w_i\tau+b_i)}\right)^{-5} - 36e^{-3(w_i\tau+b_i)} \left(1+e^{-(w_i\tau+b_i)}\right)^{-4} \\ +14e^{-2(w_i\tau+b_i)} \left(1+e^{-(w_i\tau+b_i)}\right)^{-3} - e^{-(w_i\tau+\gamma_i)} \left(1+e^{-(w_i\tau+\gamma_i)}\right)^{-2} \end{array}\right),
\end{aligned} \quad \textbf{(4)}$$

where the respective weights are $\boldsymbol{l} = [l_1, l_2, l_3, ..., l_m]$, $\boldsymbol{w} = [w_1, w_2, w_3, ..., w_m]$ and $\boldsymbol{b} = [b_1, b_2, b_3, ...b_m]$. In order to find the solution of FO-MS-NEF model given in equation (3), an objective based error function is defined as:

$$E_{Fit} = E_{Fit-1} + E_{Fit-2}, \quad \textbf{(5)}$$

where E_{Fit-1} and E_{Fit-2} are an unsupervised error functions associated to singular FO-MS-NEF model and initial conditions given in equation (3) written as:

$$E_{Fit-1} = \frac{1}{N} \sum_{k=1}^{N} \left(\frac{d^4\hat{U}_k}{d\tau_k^4} + \Psi_1 \tau_k^{-1} \frac{d^3\hat{U}_k}{d\tau_k^3} + \Psi_2 \tau_k^{-2} \frac{d^2\hat{U}_k}{d\tau_k^2} + \Psi_3 \tau_k^{-3} \frac{d\hat{U}_k}{d\tau_k} + h_k g(\hat{U}_k) \right)^2, \quad \textbf{(6)}$$

$$E_{Fit-2} = \frac{1}{4} \left((\hat{U}_0 - a)^2 + \left(\frac{d\hat{U}_0}{d\tau_k}\right)^2 + \left(\frac{d^2\hat{U}_0}{d\tau_k^2}\right)^2 + \left(\frac{d^3\hat{U}_0}{d\tau_k^3}\right)^2 \right), \quad \textbf{(7)}$$

where $Nh = 1$, $\hat{U}_k = \hat{U}(\tau_k)$, $\tau_k = kh$ and $h_k = h(\tau_k)$, where As h shows the step size, $\hat{U}_k = \hat{U}(\tau_k)$ indicates the approximate solutions of U for the k_{th} input grid point.

2.2. Optimization: ANN-PSO-AS scheme

The optimization technique to solve the FO-MS-NEF system given in equation (3) is developed by the structure of hybrid-computing PSO-AS scheme.

PSO is a global search scheme and applied as an optimization process. It is an efficient approach due to its tremendous features like decentralization, self-organization and collective behavior based on swarm intelligence, and the inspiration comes from the biological system including bird flocking, animal herding, ant colonies, fish schooling, hawks hunting and microbial intelligence. PSO proposed by Kennedy et al in the last century and used as an alteration of a famous global search genetic algorithm [49]. The implementation process of the PSO is very easy due to the less memory requirements.

In the theory of search space, an applicant outcome by applying the optimization procedure is known as a particle. In PSO scheme, the initial swarms expands in a wider domain. The refinement of the PSO provides optimal iterative results $\boldsymbol{P}_{LB}^{\varphi-1}$ and $\boldsymbol{P}_{GB}^{\varphi-1}$ that indicates the swarm's position and velocity, mathematically given as:

$$\boldsymbol{X}_i^{\varphi} = \boldsymbol{X}_i^{\varphi-1} + \boldsymbol{V}_i^{\varphi-1}, \tag{8}$$

$$\boldsymbol{V}_i^{\varphi} = \psi \boldsymbol{V}_i^{\varphi-1} + \varphi_1 (\boldsymbol{P}_{LB}^{\varphi-1} - \boldsymbol{X}_i^{\varphi-1}) \boldsymbol{r}_1 + \varphi_2 (\boldsymbol{P}_{GB}^{\varphi-1} - \boldsymbol{X}_i^{\varphi-1}) \boldsymbol{r}_2, \tag{9}$$

where $\boldsymbol{X}_i$ and $\boldsymbol{V}_i$ are the position and velocity, ψ represents the inertia vector. While, φ_1 and φ_2 are the values of the constant acceleration. PSO has wide-ranging applications in circuit theory [50], parameter estimation for the generalized gamma distribution [51], nonlinear benchmark model represented with system of nonlinear equations [52], bound-constrained nonlinear optimization problems [53] and estimation problem of undrained shear strength of soil [54]. The global search scheme PSO rapidly converges using the hybridization with an appropriate local search scheme by taking the best PSO standards as a primary weight. Subsequently, an operative local search technique based on active-set (AS) approach is applied for better refinement of the outcomes accomplished by the proposed optimization scheme. Active set method determines the local search space by limiting the constraints, which stimulus the final optimal results. The efficient hybridization with the local search scheme reduces the complexity of the results due to well-organized estimation of AS method. Recently, this method has been used in the optimization of predictive control models [55], linearly constrained non-Lipschitz nonconvex optimization tasks [56], optimization mechanism in pricing American better-off option on two assets [57], nonlinear tasks associated with-monotone operators [58] and embedded model predictive control problems [59]. In this research study, the hybrid of PSO-AS scheme is applied to solve the FO-MS-NEF model given in equation (3). The detailed pseudocode is provided in Table 1 that is based on ANN-PSO-AS scheme.

3. Performance measures

In this study, the statistical measures of Theil's inequality coefficient (TIC), Variance Account for (VAF) and Nash Sutcliffe Efficiency (NSE) are presented for solving three different variants of FO-MS-NEF model. The mathematical symbolizations of these statistical based operators are given as:

$$\text{TIC} = \frac{\sqrt{\frac{1}{n}\sum_{i=1}^{n}\left(U_i - \hat{U}_i\right)^2}}{\left(\sqrt{\frac{1}{n}\sum_{i=1}^{n}U_i^2} + \sqrt{\frac{1}{n}\sum_{i=1}^{n}\hat{U}_i^2}\right)}, \tag{10}$$

$$\begin{cases} VAF = \left(1 - \dfrac{\operatorname{var}\left(U_i(x) - \hat{U}_i(x)\right)}{\operatorname{var}\left(U_i(x)\right)}\right) * 100, \\ EVAF = \left|VAF - 100\right|. \end{cases} \quad (11)$$

$$\begin{cases} \text{NSE} = 1 - \dfrac{\sum_{i=1}^{n}\left(U_i - \hat{U}_i\right)^2}{\sum_{i=1}^{n}\left(\hat{U}_i - \bar{U}_i\right)^2}, \qquad \bar{U}_i = \dfrac{1}{n}\sum_{i=1}^{n} U_i, \\ \text{ENSE} = 1 - \text{NSE}. \end{cases} \quad (12)$$

Table 1: Method of optimization using the ANN-PSO-AS algorithm

Start of PSO

Step 1: **'Initialization'**: Produce the initial swarm arbitrarily. Modify the 'PSO' parameters and 'optimoptions' routine.

Step 2: **Formulation of Fitness**: Examine the 'fitness values' of each particle using equation (5).

Step 3: **'Ranking'**: Rank each particle for minimum values of 'fit function'.

Step 4: **Terminating Standards**: Stop if 'Fitness level' accomplished or to execute the selected 'flights/cycles' When 'stopping' standards meet, then go to Step 5

Step 5: **'Renewal'**: Using Equations (8) and (9), call the 'position' and 'velocity'

Step 6: **'Improvement'**: Repeat from step (2)-(6) until the whole 'flights' are attained.

Step 7: **'Storage'**: Save the best achieved 'fit values', represented as 'best global particle'

PSO algorithm Ends

Start the PSO-AS algorithm

Inputs: Best global values of the particle"

Output: $\mathbf{W}_{PSO-AS}$ denotes the best values of the PSO-AS algorithm

Initialize: Start point is $\mathbf{W}_{PSO}$ (Global best values)

Termination: Stop if {Fitness= E_{Fit} =10^{-18}},{Iterations=1800}, {TolFun= TolX = TolCon = 10^{-21}} and {MaxFunEvals = 280000} the above standards obtained.

While {Terminate}

Fitness calculation: For the 'fitness values' E_{Fit}, use the equation (5)

Adjustments: Invoke the routine of 'fmincon' for the AS scheme to adjust the values of the 'weight vector'.

Move to 'fitness step' using the 'weight's vector' updated form.

Store: Save the $\mathbf{W}_{PSO-AS}$, generations, E_{Fit}, time and function count for the current trial.

PSO-AS algorithm Ends

4. Results and discussions

In this section, the detailed results and simulations are provided for solving the three different variants based on FO-MS-NEF model.

Example-1: Consider a highly nonlinear FO-MS-NEF model-based equation is given as:

$$\begin{aligned}&\frac{d^4U}{d\tau^4}+\frac{3}{\tau}\frac{d^3U}{d\tau^3}-96(5\tau^8-10\tau^4+1)e^{-4U}=0,\\&U(0)=\frac{dU(0)}{d\tau}=0,\frac{d^2U(0)}{d\tau^2}=\frac{d^3U(0)}{d\tau^3}=0.\end{aligned}\tag{13}$$

The true solution of equation (13) is $\log\left(1+\tau^4\right)$, while the corresponding objective function becomes as:

$$\begin{aligned}E_{Fit}=&\frac{1}{N}\sum_{k=1}^{N}\left(\tau_k\frac{d^4\hat{U}_k}{d\tau_k^4}+3\frac{d^3\hat{U}_k}{d\tau_k^3}-96\tau_k(5\tau_k^8-10\tau_k^4+1)e^{-4\hat{U}}\right)^2\\&+\frac{1}{4}\left((\hat{U}_0)^2+\left(\frac{d\hat{U}_0}{d\tau_k}\right)^2+\left(\frac{d^2\hat{U}_0}{d\tau_k^2}\right)^2+\left(\frac{d^3\hat{U}_0}{d\tau_k^3}\right)^2\right).\end{aligned}\tag{14}$$

Example-2: Consider the FO-MS-NEF model-based equation is given as:

$$\begin{aligned}&\frac{d^4U}{d\tau^4}+\frac{12}{\tau}\frac{d^3U}{d\tau^3}+\frac{36}{\tau^2}\frac{d^2U}{d\tau^2}+\frac{24}{\tau^3}\frac{dU}{d\tau}+60(3\tau^8-18\tau^4+7)U^9=0,\\&U(0)=1,\frac{dU(0)}{d\tau}=0,\ \frac{d^2U(0)}{d\tau^2}=\frac{d^3U(0)}{d\tau^3}=0.\end{aligned}\tag{15}$$

The true solution of equation (15) is $\frac{1}{\sqrt{1+\tau^4}}$, while the corresponding objective function becomes as:

$$\begin{aligned}E_{Fit}=&\frac{1}{N}\sum_{k=1}^{N}\left(\tau_k^3\frac{d^4\hat{U}_k}{d\tau_k^4}+12\tau_k^2\frac{d^3\hat{U}_k}{d\tau_k^3}+36\tau_k\frac{d^2\hat{U}_k}{d\tau_k^2}+24\frac{d\hat{U}_k}{d\tau_k}+60\tau_m^3(3\tau_m^8-18\tau_m^4+7)\hat{U}^9\right)^2\\&+\frac{1}{4}\left((\hat{U}_0-1)^2+\left(\frac{d\hat{U}_0}{d\tau_k}\right)^2+\left(\frac{d^2\hat{U}_0}{d\tau_k^2}\right)^2+\left(\frac{d^3\hat{U}_0}{d\tau_k^3}\right)^2\right).\end{aligned}\tag{16}$$

Example-3: Consider the FO-MS-NEF model-based equation is given as:

$$\frac{d^4U}{d\tau^4}+\frac{4}{\tau}\frac{d^3U}{d\tau^3}+\frac{2}{\tau^2}\frac{d^2U}{d\tau^2}-3(12\tau^8-53\tau^4+12)U^{-15}=0,$$
$$U(0)=1,\frac{dU(0)}{d\tau}=0,\ \frac{d^2U(0)}{d\tau^2}=\frac{d^3U(0)}{d\tau^3}=0. \quad \textbf{(17)}$$

The true/exact solution of the above equation (17) is $(1+\tau^4)^{\frac{1}{4}}$ and the corresponding objective function becomes as:

$$E_{Fit}=\frac{1}{N}\sum_{k=1}^{N}\left(\tau_k^2\frac{d^4\hat{U}_k}{d\tau_k^4}+4\tau_k\frac{d^3\hat{U}_k}{d\tau_k^3}+2\frac{d^2\hat{U}_k}{d\tau_k^2}-3\tau_m^2(12\tau_m^8-53\tau_m^4+12)\hat{U}^{-15}\right)^2$$
$$+\frac{1}{4}\left((\hat{U}_0-1)^2+\left(\frac{d\hat{U}_0}{d\tau_k}\right)^2+\left(\frac{d^2\hat{U}_0}{d\tau_k^2}\right)^2+\left(\frac{d^3\hat{U}_0}{d\tau_k^3}\right)^2\right). \quad \textbf{(18)}$$

The proposed ANN-PSO-AS algorithm for fifty independent trials to achieve the system parameter for the nonlinear FO-MS-NEF model given in equation (3). The set of the best weight is used to indicate the obtained outcomes of the equation (3), mathematically written as:

$$\hat{U}_1(\tau)=\frac{4.2709}{1+e^{-(0.865\tau+4.772)}}-\frac{0.6279}{1+e^{-(-4.462\tau+2.064)}}-\frac{6.2427}{1+e^{-(-2.167\tau+1.567)}}+...+\frac{2.1351}{1+e^{-(0.627\tau+1.742)}}, \quad \textbf{(19)}$$

$$\hat{U}_2(\tau)=\frac{0.5207}{1+e^{-(3.167\tau-3.497)}}-\frac{0.9658}{1+e^{-(1.090\tau-0.890)}}+\frac{2.3645}{1+e^{-(0.394\tau-1.190)}}+...-\frac{0.2134}{1+e^{-(1.662\tau+1.007)}}, \quad \textbf{(20)}$$

$$\hat{U}_3(\tau)=\frac{14.0022}{1+e^{-(11.257\tau+11.586)}}-\frac{0.0414}{1+e^{-(-4.242\tau+11.1332)}}-\frac{0.2207}{1+e^{-(9.020\tau+5.964)}}+...-\frac{11.2936}{1+e^{-(2.806\tau-11.782)}}. \quad \textbf{(21)}$$

The performance of optimization is provided to solve the FO-MS-NEF model-based examples 1-3 using the hybrid of PSO-AS algorithm for 50 trials. A best weight sets and comparison of the proposed/exact results of the FO-MS-NEF model-based examples 1-3 using the 10 number of neurons are provided in Figure. 1. It is seen that the proposed and exact results matched for all the examples, which shows the perfection and exactness of the proposed ANN-PSO-AS algorithm. Figure 2 shows the AE values and performance investigations for the ANN-PSO-AS algorithm for FO-MS-NEF equations 1-3. In Figure 2(a), the AE values for examples 1-3 are provided. It is observed that the AE for problem 1 and 3 lie about 10^{-04} to 10^{-05}, while in example 2, the AE lies in the 10^{-04} to 10^{-06} interval. Figure 2(b) specifies the performance indices for all the examples using Fitness, EVAF, TIC and ENSE. It is seen that for example 1-3, the fitness lie in the ranges of 10^{-07} to 10^{-08}. The TIC and EVAF gages for examples 1 and 3 are found to be 10^{-08} - 10^{-09}, while for problem 2, the TIC and EVAF gages values exist around 10^{-09} to 10^{-10}. The ENSE for examples 1 and 2 closely lie 10^{-08} to 10^{-09} interval, while in 3rd example, the ENSE are close to 10^{-07}.

Problem 1

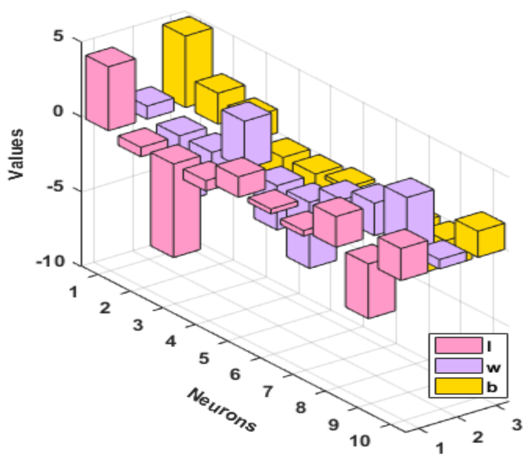

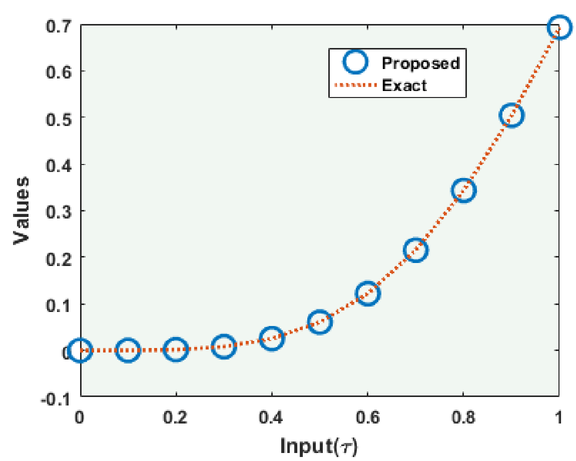

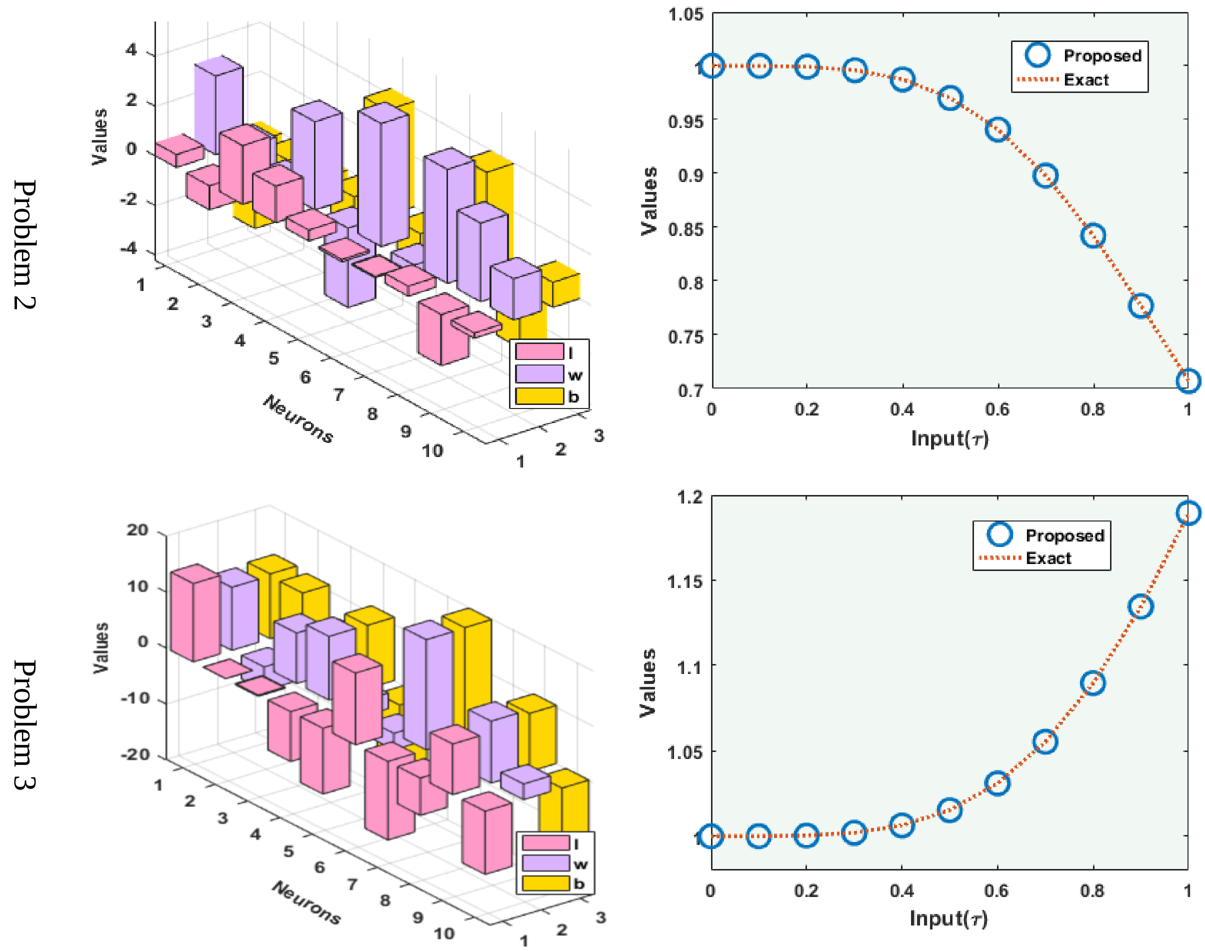

Figure 1: Best weight sets and comparison of the proposed/exact solutions of the FO-MS-NEF model-based examples 1-3 using 10 numbers of neurons

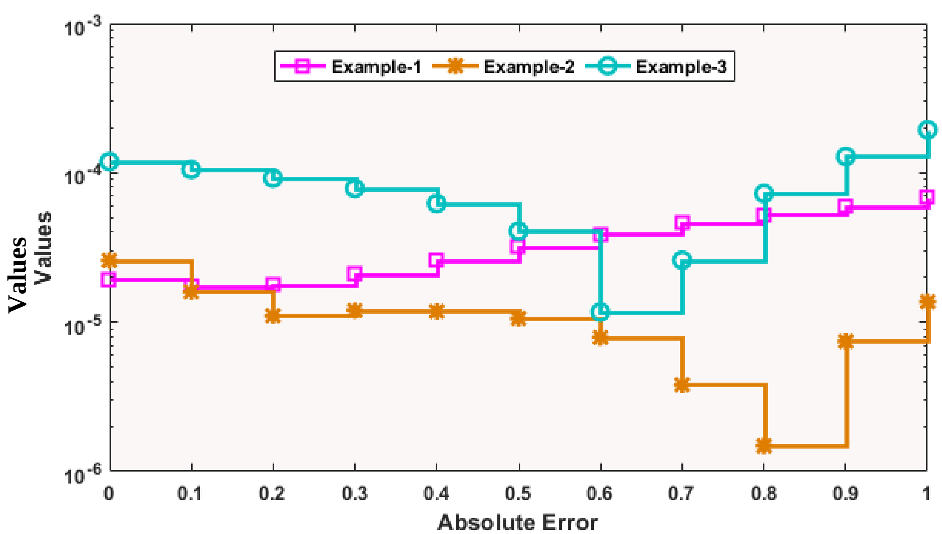

(a) Values of the AE for examples 1-3

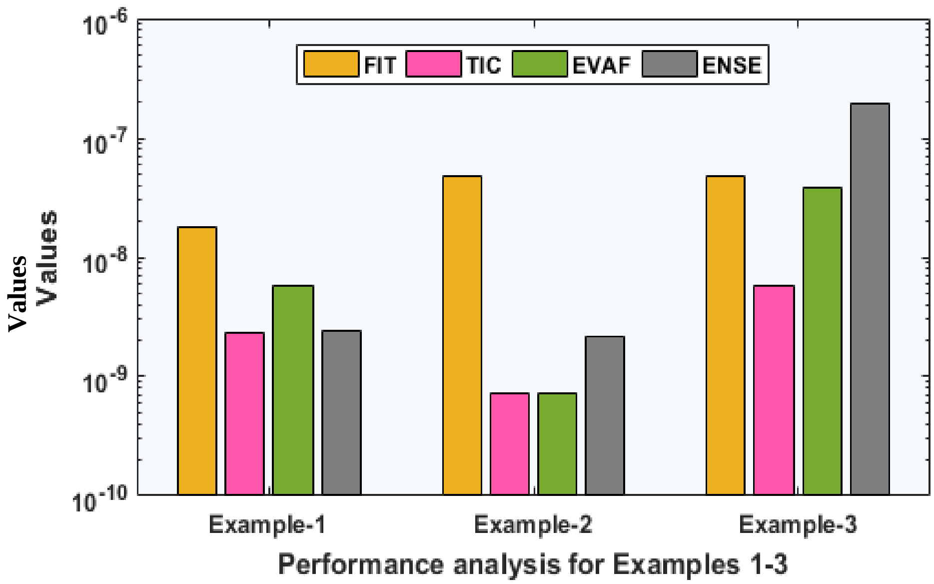

(b) Performance investigations for examples 1-3

Figure 2: AE values and performance investigations using the ANN-PSO-AS algorithm to solve the FO-MS-NEF examples 1-3

In figures 3 to 6, the convergence measures based on the values of the fitness, TIC, ENSE and EVAF attained for a number of independent trials along with the values of histogram and boxplots for the examples 1-3 are plotted. The outcomes are found to be satisfactory and one can see that almost 75% of the trials achieve accurate and precise values of the Fitness, TIC, ENSE and EVAF.

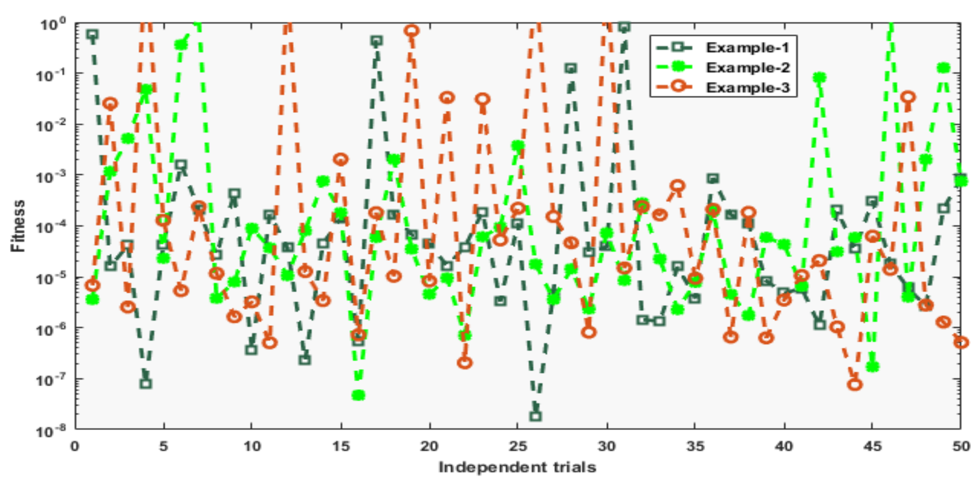

(a) Values of the Fitness in convergence analysis for examples 1-3

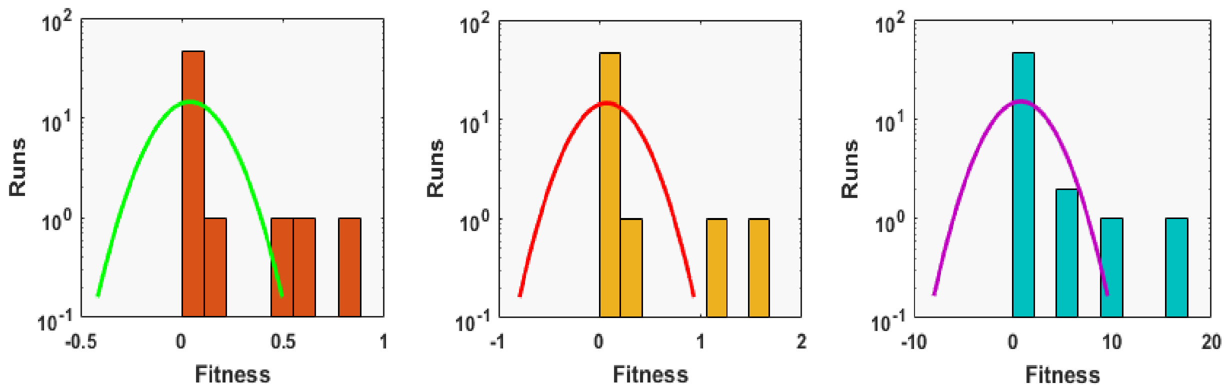

(b) Histogram of example 1 **(c) Histogram of example 2** **(d) Histogram of example 3**

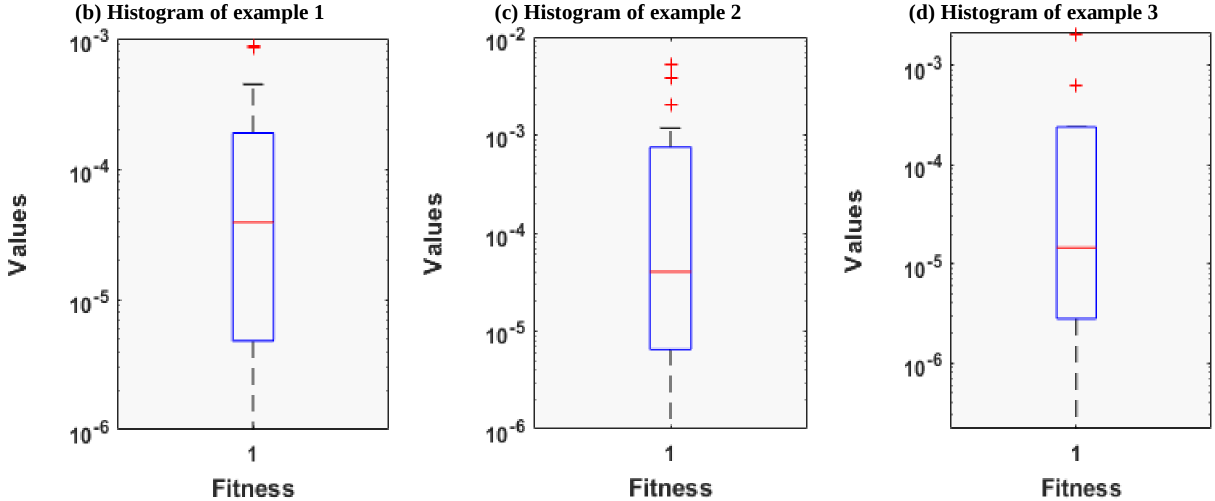

(e) Boxplot of example 1 **(f) Boxplot of example 2** **(g) Boxplot of example 3**

Figure 3: Statistical studies for the ANN-PSO-AS scheme via Fitness along with the boxplots and histograms to solve the FO-MS-NEF model-based examples 1-3

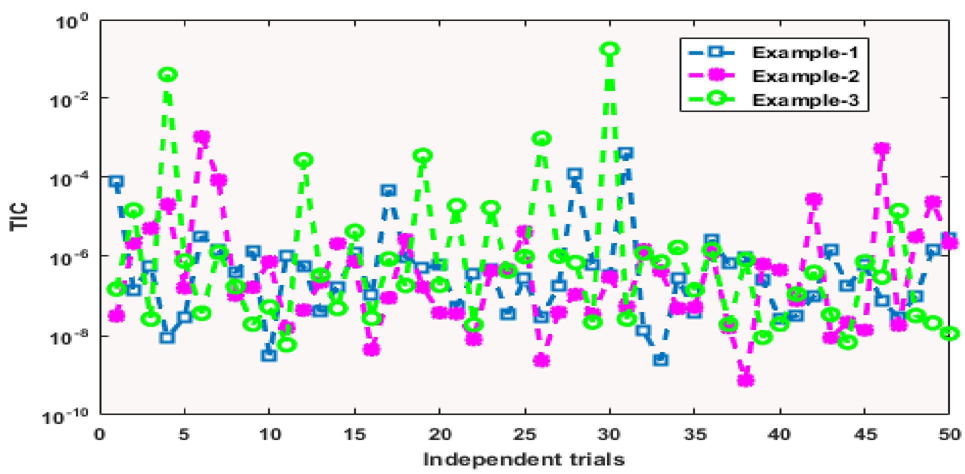

(a) Values of the TIC in convergence analysis for examples 1-3

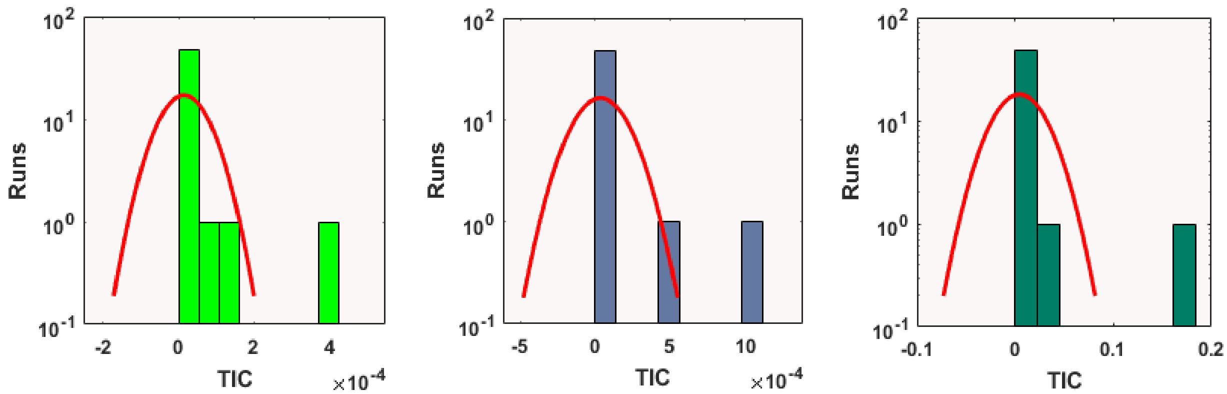

(b) Histogram of example 1 **(c) Histogram of example 2** **(d) Histogram of example 3**

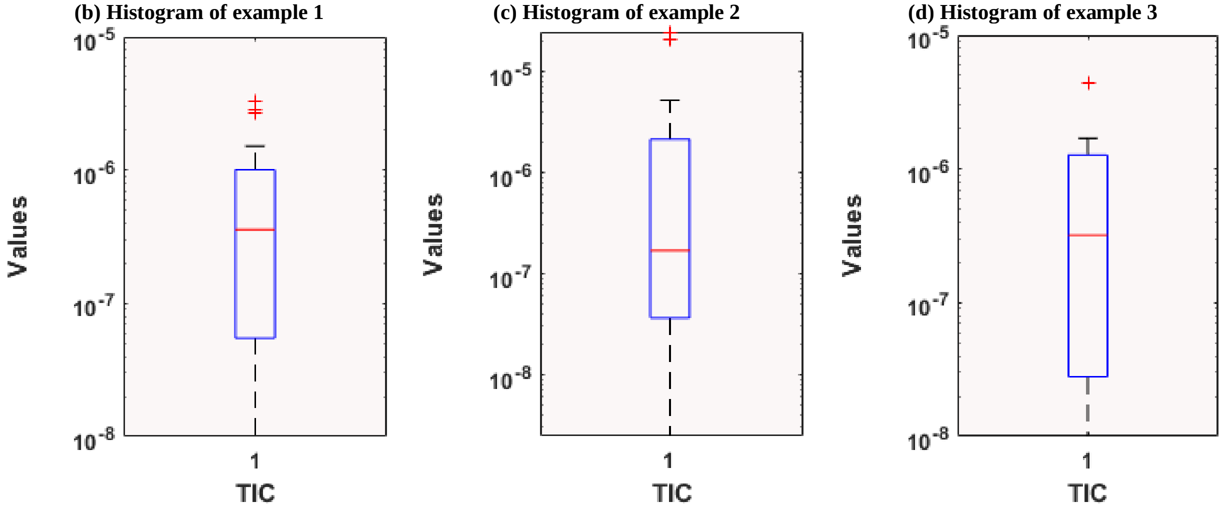

(e) Boxplot of example 1 **(f) Boxplot of example 2** **(g) Boxplot of example 3**

Figure 4: Statistical studies for the designed ANN-PSO-AS scheme via TIC along with the boxplots and histograms to solve the FO-MS-NEF model-based examples 1-3

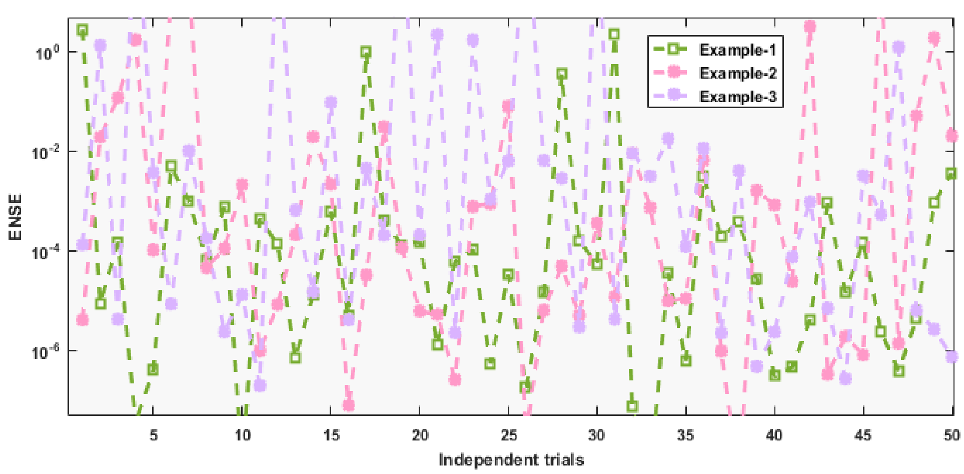

(a) Values of the ENSE in convergence analysis for examples 1-3

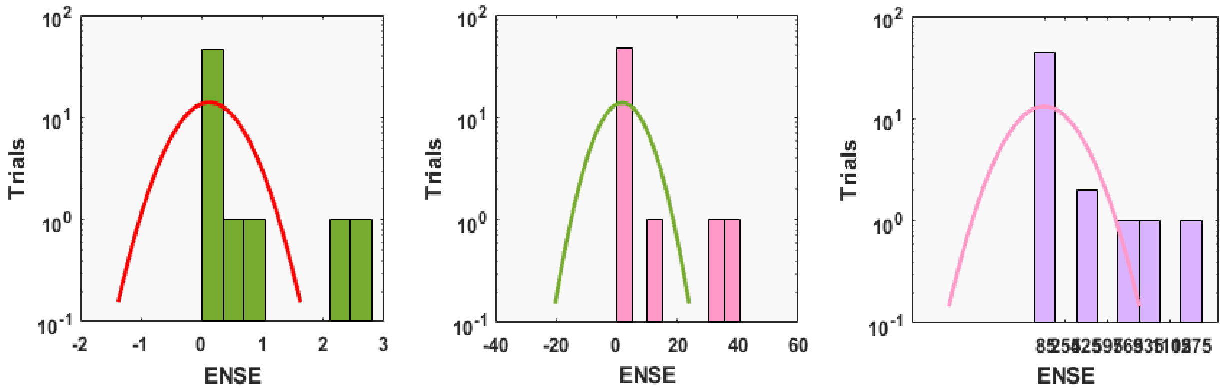

(b) Histogram of example 1 (c) Histogram of example-2 (d) Histogram of example 3

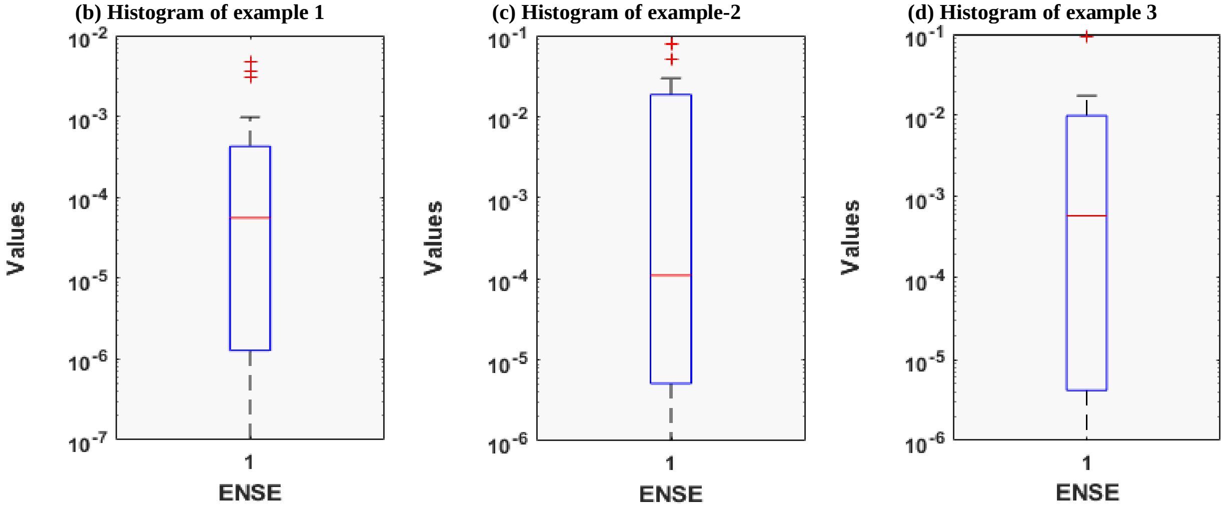

(e) Boxplot of example-1 (f) Boxplot of example 2 (g) Boxplot of example 3

Figure 5: Statistical studies for the designed ANN-PSO-AS scheme via ENSE for the boxplots and histograms to solve the FO-MS-NEF model-based examples 1-3

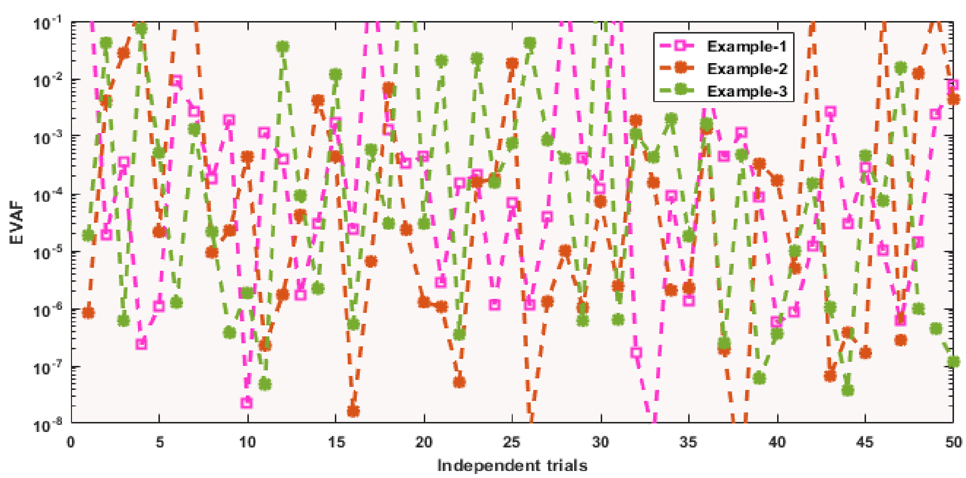

(a) Values of the EVAF in convergence analysis for examples 1-3

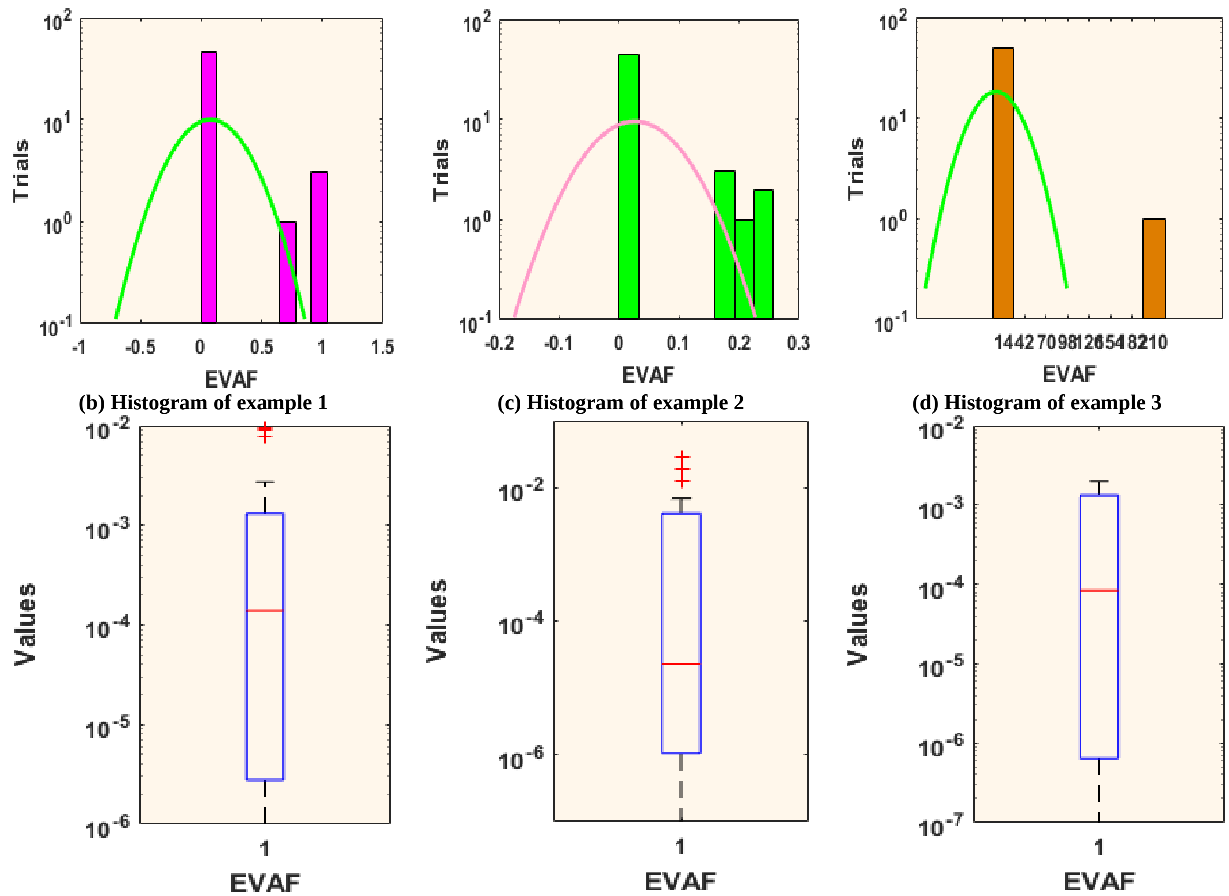

(b) Histogram of example 1 (c) Histogram of example 2 (d) Histogram of example 3

(e) Boxplot of example 1 (f) Boxplot of example 2 (g) Boxplot of example 3

Figure 6: Statistical studies for the designed ANN-PSO-AS scheme via EVAF for the boxplots and histograms to solve the FO-MS-NEF model-based examples 1-3

In order to find the statistical investigations using the ANN-PSO-AS algorithm to solve the FO-MS-NEF model based examples 1-3, statistical procedures are performed for 50 independent trials in terms of minimum (Min), Mean, median (Med) and semi interquartile range (SI-R). The mathematical notations of SI-R is $0.5(Q_3 - Q_1)$, where the first and third quartiles are Q_1 and Q_3, respectively. The statistic investigations based on the operators Min, Mean, Med and SI-R are provided in Table 2 to solve the FO-MS-NEF. These statistical values for all the operators for the examples 1-3 are found to be satisfactory, which indicates the correctness and precision of the ANN-PSO-AS algorithm.

Table 2: Statistics solutions for the FO-MS-NEF model-based Examples 1-3

τ	[Example 1]				[Example 2]				[Example 3]			
	Min	**Mean**	**Med**	**SI-R**	**Min**	**Mean**	**Med**	**SI-R**	**Min**	**Mean**	**Med**	**SI-R**
0	1.92E-05	9.82E-02	6.38E-03	8.52E-03	5.41E-06	1.31E-01	3.46E-03	2.33E-02	1.01E-04	5.29E-01	5.86E-03	1.25E-02
0.1	1.74E-05	9.82E-02	6.38E-03	8.43E-03	1.60E-05	1.31E-01	3.48E-03	2.32E-02	1.05E-04	5.35E-01	5.98E-03	1.28E-02
0.2	1.78E-05	9.79E-02	6.34E-03	8.30E-03	1.10E-05	1.31E-01	3.47E-03	2.31E-02	9.21E-05	5.44E-01	6.08E-03	1.30E-02

0.3	2.00E-05	9.70E-02	6.16E-03	8.05E-03	1.20E-05	1.30E-01	3.38E-03	2.25E-02	7.86E-05	5.59E-01	6.07E-03	1.31E-02
0.4	2.85E-06	9.48E-02	5.70E-03	7.37E-03	1.18E-05	1.28E-01	3.12E-03	2.11E-02	6.22E-05	5.79E-01	5.83E-03	1.27E-02
0.5	1.31E-05	9.04E-02	4.75E-03	6.06E-03	1.06E-05	1.24E-01	2.60E-03	1.81E-02	4.06E-05	6.02E-01	5.19E-03	1.15E-02
0.6	2.50E-06	8.30E-02	3.10E-03	3.95E-03	7.90E-06	1.18E-01	1.75E-03	1.33E-02	1.17E-05	6.29E-01	3.96E-03	9.32E-03
0.7	2.38E-05	7.21E-02	6.25E-04	7.35E-04	3.80E-06	1.09E-01	5.77E-04	6.54E-03	1.59E-05	6.57E-01	1.87E-03	5.84E-03
0.8	1.36E-05	6.36E-02	1.84E-03	3.79E-03	1.48E-06	9.91E-02	8.46E-04	1.82E-03	8.55E-06	6.88E-01	5.55E-04	1.07E-03
0.9	9.25E-06	5.64E-02	6.43E-03	1.01E-02	7.44E-06	9.53E-02	2.40E-03	1.12E-02	8.50E-05	7.24E-01	4.25E-03	4.81E-03
1	2.61E-05	5.42E-02	1.16E-02	1.62E-02	1.37E-05	9.23E-02	4.00E-03	2.10E-02	1.80E-04	7.64E-01	8.66E-03	1.25E-02

5. Conclusion

The present work is to investigate the numerical outcomes of the multi-singular fourth order nonlinear Emden-Fowler equations using an accurate, steady, stable, reliable and consistent by functioning the ANNs strength with continuous mapping. An objective function is optimized by applying the local and global abilities of particle swarm optimization along with the active-set algorithm. The proposed ANN-PSO-AS scheme is executed to solve three different problems of the multi-singular fourth order nonlinear Emden-Fowler equations. The accurate and reliable performance is experiential for ANN-PSO-AS scheme on the basis of absolute error with dependable accuracy, which is observed around 5 to 6 decimals of accurateness from the current exact/true results for all the problems of the nonlinear multi-singular fourth order Emden-Fowler equations. Furthermore, the statistical explanations are also considering using Min, Mean, Med, and SI-R procedures to authenticate the convergence, robustness and accuracy of the designed ANN-PSO-AS algorithm to solve the nonlinear fourth order multi-singular Emden-Fowler model. It is observed that a reliable values have been calculated using these procedures.

One may investigate to extend the presented ANN-PSO-AS approach with the introduction of fractional neural networks [60-63], fractional evolutionary/swarming optimization [65-70] mechanism or combination of the both for solving the nonlinear higher order systems [71-73].

References

[1] Wong, J.S., 1975. On the generalized Emden–Fowler equation. *Siam Review*, *17*(2), pp.339-360.

[2] Wazwaz, A.M., 2005. Adomian decomposition method for a reliable treatment of the Emden–Fowler equation. *Applied Mathematics and Computation*, *161*(2), pp.543-560.

[3] Rach, R., Duan, J. S. and Wazwaz, A. M., 2014. Solving coupled Lane–Emden boundary value problems in catalytic diffusion reactions by the Adomian decomposition method. Journal of Mathematical Chemistry, 52(1), pp. 255-267.

[4] Taghavi, A., Pearce, S., 2013. A solution to the Lane–Emden equation in the theory of stellar structure utilizing the Tau method. Mathematical Methods in the Applied Sciences, 36(10), pp.1240-1247.

[5] Boubaker, K. and Van Gorder, R.A., 2012. Application of the BPES to Lane–Emden equations governing polytropic and isothermal gas spheres. New Astronomy, 17(6), pp. 565-569.

[6] Rach, R., Duan, J. S. and Wazwaz, A. M., 2014. Solving coupled Lane–Emden boundary value problems in catalytic diffusion reactions by the Adomian decomposition method. Journal of Mathematical Chemistry, 52(1), pp. 255-267

[7] Khan, J. A., et al., 2015. Nature-inspired computing approach for solving non-linear singular Emden–Fowler problem arising in electromagnetic theory. Connection Science, 27(4), pp. 377-396.

[8] Džurina, J., Grace, S.R., Jadlovská, I. and Li, T., 2019. Oscillation criteria for second-order Emden–Fowler delay differential equations with a sublinear neutral term. *Mathematische Nachrichten*.

[9] Kosaka, A. and Miyamoto, Y., 2019. The Emden–Fowler equation on a spherical cap of Sn. *Nonlinear Analysis*, *178*, pp.110-132.

[10] Guha, P., 2020. Generalized Emden–Fowler equations in noncentral curl forces and first integrals. *Acta Mechanica*, *231*(2), pp.815-825.

[11] Pikulin, S.V., 2019. The Thomas–Fermi Problem and Solutions of the Emden–Fowler Equation. *Computational Mathematics and Mathematical Physics*, *59*(8), pp.1292-1313.

[12] Singh, K., Verma, A.K. and Singh, M., 2020. Higher order Emden–Fowler type equations via uniform Haar Wavelet resolution technique. *Journal of Computational and Applied Mathematics*, p.112836.

[13] Sabir, Z., et al., 2020. Novel design of Morlet wavelet neural network for solving second order Lane–Emden equation. Mathematics and Computers in Simulation, 172, pp.1-14

[14] Adel, W. and Sabir, Z., 2020. Solving a new design of nonlinear second-order Lane–Emden pantograph delay differential model via Bernoulli collocation method. The European Physical Journal Plus, 135(6), p.427. 4-100.

[15] Sabir, Z., Saoud, S., Raja, M.A.Z., Wahab, H.A. and Arbi, A., 2020. Heuristic computing technique for numerical solutions of nonlinear fourth order Emden–Fowler equation. Mathematics and Computers in Simulation.

[16] Singh, R., 2019. Analytic solution of singular Emden-Fowler-type equations by Green's function and homotopy analysis method. *The European Physical Journal Plus*, *134*(11), p.583.

[17] Sabir, Z., Günerhan, H. and Guirao, J.L., 2020. On a new model based on third-order nonlinear multisingular functional differential equations. Mathematical Problems in Engineering, 2020.

[18] Asadpour, S., Yazdani Cherati, A. and Hosseinzadeh, H., 2019. Solving the general form of the Emden-Fowler equations with the Moving Least Squares method. *Journal of Mathematical Modeling*, *7*(2), pp.231-250.

[19] Moaaz, O., Elabbasy, E.M. and Qaraad, B., 2020. An improved approach for studying oscillation of generalized Emden–Fowler neutral differential equation. *Journal of Inequalities and Applications*, *2020*(1), pp.1-18.

[20] Sabir, Z., Amin, F., Pohl, D. and Guirao, J.L., Intelligence computing approach for solving second order system of Emden–Fowler model. Journal of Intelligent & Fuzzy Systems, (Preprint), pp.1-16.

[21] Yadav, N., Yadav, A., Kumar, M. and Kim, J.H., 2017. An efficient algorithm based on artificial neural networks and particle swarm optimization for solution of nonlinear Troesch's problem. Neural Computing and Applications, 28(1), pp.171-178.

[22] Sabir, Z., Umar, M., Guirao, J.L., Shoaib, M. and Raja, M.A.Z., 2020. Integrated intelligent computing paradigm for nonlinear multi-singular third-order Emden–Fowler equation. Neural Computing and Applications, pp.1-20.

[23] İnce, N. and Shamilov, A., 2020. An Application of New Method to Obtain Probability Density Function of Solution of Stochastic Differential Equations. Applied Mathematics and Nonlinear Sciences, 5(1), pp.337-348.

[24] Sabir, Z., Baleanu, D., Shoaib, M. and Raja, M.A.Z., 2020. Design of stochastic numerical solver for the solution of singular three-point second-order boundary value problems. Neural Computing and Applications, pp.1-17.

[25] Sagna, Y., 2019. Multidimensional BSDE with Poisson jumps of Osgood type. Applied Mathematics and Nonlinear Sciences, 4(2), pp.387-394.

[26] Masood, Z., et al., 2017. Design of Mexican Hat Wavelet neural networks for solving Bratu type nonlinear systems. *Neurocomputing*, *221*, pp.1-14.

[27] Raja, M.A.Z., Samar, R., Alaidarous, E.S. and Shivanian, E., 2016. Bio-inspired computing platform for reliable solution of Bratu-type equations arising in the modeling of electrically conducting solids. *Applied Mathematical Modelling*, *40*(11-12), pp.5964-5977.

[28] Bukhari, A.H., et al., 2020. Fractional Neuro-Sequential ARFIMA-LSTM for Financial Market Forecasting. *IEEE Access*.

[29] Raja, M.A.Z., Manzar, M.A., Shah, S.M. and Chen, Y., 2020. Integrated Intelligence of Fractional Neural Networks and Sequential Quadratic Programming for Bagley–Torvik Systems Arising in Fluid Mechanics. *Journal of Computational and Nonlinear Dynamics*, *15*(5).

[30] Bukhari, A.H., et al., 2020. Neuro-fuzzy modeling and prediction of summer precipitation with application to different meteorological stations. *Alexandria Engineering Journal*, *59*(1), pp.101-116.

[31] Umar, M., et al., 2019. Intelligent computing for numerical treatment of nonlinear prey–predator models. Applied Soft Computing, 80, pp.506-524.

[32] Ahmad, I., et al., 2019. Novel applications of intelligent computing paradigms for the analysis of nonlinear reactive transport model of the fluid in soft tissues and microvessels. *Neural Computing and Applications*, *31*(12), pp.9041-9059.

[33] Sabir, Z., et al., 2018. Neuro-heuristics for nonlinear singular Thomas-Fermi systems. Applied Soft Computing, 65, pp.152-169.

[34] Sabir, Z., Raja, M.A.Z., Guirao, J.L. and Shoaib, M., A neuro-swarming intelligence based computing for second order singular periodic nonlinear boundary value problems.

[35] Mehmood, A., et al., 2019. Integrated computational intelligent paradigm for nonlinear electric circuit models using neural networks, genetic algorithms and sequential quadratic programming. *Neural Computing and Applications*, https://doi.org/10.1007/s00521-019-04573-3

[36] Raja, M.A.Z., Mehmood, J., Sabir, Z., Nasab, A.K. and Manzar, M.A., 2019. Numerical solution of doubly singular nonlinear systems using neural networks-based integrated intelligent computing. Neural Computing and Applications, 31(3), pp.793-812.

[37] Fateh, M.F., et al., 2019. Differential evolution based computation intelligence solver for elliptic partial differential equations. *Frontiers of Information Technology & Electronic Engineering*, *20*(10), pp.1445-1456.

[38] Umar, M., Sabir, Z., Amin, F., Guirao, J.L. and Raja, M.A.Z., 2020. Stochastic numerical technique for solving HIV infection model of CD4+ T cells. The European Physical Journal Plus, 135(6), p.403.

[39] Sabir, Z., Wahab, H.A., Umar, M. and Erdoğan, F., 2019. Stochastic numerical approach for solving second order nonlinear singular functional differential equation. Applied Mathematics and Computation, 363, p.124605.

[40] Sabir, Z., Raja, M.A.Z., Umar, M. and Shoaib, M., 2020. Neuro-swarm intelligent computing to solve the second-order singular functional differential model. The European Physical Journal Plus, 135(6), p.474.

[41] Umar, M., et al,. 2019. Unsupervised constrained neural network modeling of boundary value corneal model for eye surgery. Applied Soft Computing, 85, p.105826.

[42] Raja, M.A.Z., Umar, M., Sabir, Z., Khan, J.A. and Baleanu, D., 2018. A new stochastic computing paradigm for the dynamics of nonlinear singular heat conduction model of the human head. The European Physical Journal Plus, 133(9), p.364.

[43] Umar, M., Raja, M.A.Z., Sabir, Z., Alwabli, A.S. and Shoaib, M., 2020. A stochastic computational intelligent solver for numerical treatment of mosquito dispersal model in a heterogeneous environment. The European Physical Journal Plus, 135(7), pp.1-23.

[44] Mehmood, A., et al., 2019. Integrated intelligent computing paradigm for the dynamics of micropolar fluid flow with heat transfer in a permeable walled channel. *Applied Soft Computing*, *79*, pp.139-162.

[45] Raja, M.A.Z., Mehmood, A., Khan, A.A. and Zameer, A., 2019. Integrated intelligent computing for heat transfer and thermal radiation-based two-phase MHD nanofluid flow model. *Neural Computing and Applications*, pp.1-33.

[46] Liu, Z., Yang, Y. and Cai, Q., 2019. Neural network as a function approximator and its application in solving differential equations. *Applied Mathematics and Mechanics*, *40*(2), pp.237-248.

[47] Sun, H., Hou, M., Yang, Y., Zhang, T., Weng, F. and Han, F., 2019. Solving partial differential equation based on Bernstein neural network and extreme learning machine algorithm. *Neural Processing Letters*, *50*(2), pp.1153-1172.

[48] Avrutskiy, V.I., 2020. Neural networks catching up with finite differences in solving partial differential equations in higher dimensions. *Neural Computing and Applications*, pp.1-16.

[49] Zameer, A., et al., 2017. Intelligent and robust prediction of short term wind power using genetic programming based ensemble of neural networks. *Energy conversion and management*, *134*, pp.361-372.

[50] Mehmood, A., et al., 2019. Design of nature-inspired heuristic paradigm for systems in nonlinear electrical circuits. Neural Computing and Applications, pp.1-17.

[51] Özsoy, V.S., Ünsal, M.G. and Örkcü, H.H., 2020. Use of the heuristic optimization in the parameter estimation of generalized gamma distribution: comparison of GA, DE, PSO and SA methods. Computational Statistics, pp.1-31.

[52] Raja, M.A.Z., Zameer, A., Kiani, A.K., Shehzad, A. and Khan, M.A.R., 2018. Nature-inspired computational intelligence integration with Nelder–Mead method to solve nonlinear benchmark models. *Neural Computing and Applications*, *29*(4), pp.1169-1193.

[53] Duary, A., Rahman, M.S., Shaikh, A.A., Niaki, S.T.A. and Bhunia, A.K., 2020. A new hybrid algorithm to solve bound-constrained nonlinear optimization problems. Neural Computing and Applications, pp.1-26.

[54] Pham, B.T., Qi, C., Ho, L.S., Nguyen-Thoi, T., Al-Ansari, N., Nguyen, M.D., Nguyen, H.D., Ly, H.B., Le, H.V. and Prakash, I., 2020. A Novel Hybrid Soft Computing Model Using Random Forest and Particle Swarm Optimization for Estimation of Undrained Shear Strength of Soil. Sustainability, 12(6), p.2218.

[55] Koehler, S., Danielson, C. and Borrelli, F., 2017. A primal-dual active-set method for distributed model predictive control. Optimal Control Applications and Methods, 38(3), pp. 399-419.

[56] Zhang, C. and Chen, X., 2020. A Smoothing Active Set Method for Linearly Constrained Non-Lipschitz Nonconvex Optimization. *SIAM Journal on Optimization*, *30*(1), pp.1-30.

[57] Gao, Y., Song, H., Wang, X. and Zhang, K., 2020. Primal-dual active set method for pricing American better-of option on two assets. *Communications in Nonlinear Science and Numerical Simulation*, *80*, p.104976.

[58] He, X. and Yang, P., 2019. The Primal-Dual Active Set Method for a Class of Nonlinear Problems with-Monotone Operators. *Mathematical Problems in Engineering*, *2019*.

[59] Klaučo, M., Kalúz, M. and Kvasnica, M., 2019. Machine learning-based warm starting of active set methods in embedded model predictive control. *Engineering Applications of Artificial Intelligence*, *77*, pp.1-8.

[60] Lodhi, S., Manzar, M.A. and Raja, M.A.Z., 2019. Fractional neural network models for nonlinear Riccati systems. *Neural Computing and Applications*, *31*(1), pp.359-378.

[61] Raja, M.A.Z., Samar, R., Manzar, M.A. and Shah, S.M., 2017. Design of unsupervised fractional neural network model optimized with interior point algorithm for solving Bagley–Torvik equation. *Mathematics and Computers in Simulation*, *132*, pp.139-158.

[62] Zúñiga-Aguilar, C.J., Romero-Ugalde, H.M., Gómez-Aguilar, J.F., Escobar-Jiménez, R.F. and Valtierra-Rodríguez, M., 2017. Solving fractional differential equations of variable-order involving operators with Mittag-Leffler kernel using artificial neural networks. *Chaos, Solitons & Fractals*, *103*, pp.382-403.

[63] Zúñiga-Aguilar, C.J., Coronel-Escamilla, A., Gómez-Aguilar, J.F., Alvarado-Martínez, V.M. and Romero-Ugalde, H.M., 2018. New numerical approximation for solving fractional delay differential

equations of variable order using artificial neural networks. *The European Physical Journal Plus*, *133*(2), p.75.

[65] Akbar, S., et al., 2019. Novel application of FO-DPSO for 2-D parameter estimation of electromagnetic plane waves. *Neural Computing and Applications*, *31*(8), pp.3681-3690.

[66] Muhammad, Y., et al., 2019. Design of fractional swarming strategy for solution of optimal reactive power dispatch. *Neural Computing and Applications*, https://doi.org/10.1007/s00521-019-04589-9

[67] Zameer, A., Muneeb, M., Mirza, S.M. and Raja, M.A.Z., 2020. Fractional-order particle swarm based multi-objective PWR core loading pattern optimization. *Annals of Nuclear Energy*, *135*, p.106982.

[68] Yousri, D., Abd Elaziz, M. and Mirjalili, S., 2020. Fractional-order calculus-based flower pollination algorithm with local search for global optimization and image segmentation. *Knowledge-Based Systems*, p.105889.

[69] Yousri, D. and Mirjalili, S., 2020. Fractional-order cuckoo search algorithm for parameter identification of the fractional-order chaotic, chaotic with noise and hyper-chaotic financial systems. *Engineering Applications of Artificial Intelligence*, *92*, p.103662.

[70] Yousri, D., Thanikanti, S.B., Allam, D., Ramachandaramurthy, V.K. and Eteiba, M.B., 2020. Fractional chaotic ensemble particle swarm optimizer for identifying the single, double, and three diode photovoltaic models' parameters. *Energy*, *195*, p.116979.

[71] El-Borhamy, M. and Mosalam, N., 2020. On the existence of periodic solution and the transition to chaos of Rayleigh-Duffing equation with application of gyro dynamic. Applied Mathematics and Nonlinear Sciences, 5(1), pp.93-108.

[72] Sene, N. and Abdelmalek, K., 2020. Nonlinear sub-diffusion and nonlinear sub-diffusion dispersion equations and their proposed solutions. Applied Mathematics and Nonlinear Sciences, 5(1), pp.221-236.

[73] Ziane, D., Cherif, M.H., Cattani, C. and Belghaba, K., 2019. Yang-laplace decomposition method for nonlinear system of local fractional partial differential equations. Applied Mathematics and Nonlinear Sciences, 4(2), pp.489-502.